UDC 621.3 https://doi.org/10.20998/2074-272X.2024.2.03

M. Aissaoui, H. Bouzeria, M. Benidir, M.A. Labed

Harmonics suppression in high-speed railway via single-phase traction converter with an LCL filter using fuzzy logic control strategy

Introduction. *The railway Traction Power Supply System (TPSS) encounters a common challenge related to high-frequency harmonic resonance, especially when employing AC-DC-AC traction drive systems in high-speed trains. This resonance issue arises when the harmonic elements introduced by the traction AC-DC converter on the grid side of trains align with the innate resonance frequency of the TPSS.* ***The novelty*** *the proposed work focuses on the challenges associated with resonance elevation and high-frequency harmonics in high-speed trains, while simultaneously enhancing energy quality. This is achieved by integrating a pulse-width-modulated converter on the grid side with a single-phase configuration and incorporating an LCL filter.* ***Methodology.*** *In order to optimize the system's efficiency, a robust control system is employed, taking advantage of the capabilities of a fuzzy logic controller (FLC). The choice of the FLC is justified by its straightforward design and reliability, emphasizing the dedication to precise control, as fuzzy logic excels in handling complex, nonlinear systems. Through the use of linguistic variables and heuristic reasoning, the FLC adjusts to dynamic changes in the system, demonstrating its efficacy in enhancing both transient and steady-state responses.* ***Practical value.*** *A grid-side LCL filter-based converter was meticulously designed and rigorously simulated using the MATLAB/Simulink platform. The inclusion of an advanced FLC in the system introduced a novel approach to control strategies, surpassing the traditional PI controller. Through a comprehensive comparative analysis, the simulation results showcased the remarkable efficacy of the proposed solution in an effectively mitigating high-frequency resonance within the TPSS. This outcome underscores the potential of FLC as a sophisticated control mechanism for enhancing the performance systems in railway applications, showcasing its superiority over conventional control methods. The study contributes in shedding light on innovative approaches for optimizing the control and efficiency of grid-side LCL filter-based converters in high-speed train systems.* References 33, table 2, figures 16.

Key words: **grid-side converter, LCL filter, harmonics, power quality, fuzzy logic controller, simulation, high-speed rail.**

Вступ. *Система тягового електропостачання залізниць (TPSS) стикається із загальною проблемою, пов'язаною з високочастотним гармонійним резонансом, особливо при використанні систем тягового приводу змінного, постійного та змінного струму у високошвидкісних поїздах. Ця проблема резонансу виникає, коли гармонійні елементи, що вносяться тяговим перетворювачем змінного струму в постійний струм на стороні мережі поїздів, збігаються із внутрішньою резонансною частотою TPSS.* ***Новизна*** *запропонованої роботи зосереджена на проблемах, пов'язаних із підвищенням резонансу та високочастотними гармоніками у високошвидкісних поїздах, при одночасному підвищенні якості енергії. Це досягається за рахунок інтеграції перетворювача з широтно-імпульсною модуляцією на стороні мережі з однофазною конфігурацією і включення фільтра LCL.* ***Методологія***. *Для оптимізації ефективності системи використовується надійна система управління, яка використовує можливості контролера нечіткої логіки (FLC). Вибір FLC виправданий його простою конструкцією та надійністю, що підкреслюють прихильність до точного управління, оскільки нечітка логіка чудово справляється зі складними нелінійними системами. Завдяки використанню лінгвістичних змінних та евристичних міркувань, FLC пристосовується до динамічних змін у системі, демонструючи свою ефективність у посиленні як перехідних, так і стійких реакцій.* ***Практична цінність***. *Перетворювач на основі LCL-фільтра на стороні мережі ретельно спроектований та ретельно змодельований за допомогою платформи MATLAB/Simulink. Включення до системи вдосконаленого FLC представило новий підхід до стратегій управління, що перевершує традиційний ПІ-регулятор. Завдяки всебічному порівняльному аналізу, результати моделювання продемонстрували чудову ефективність запропонованого рішення в ефективному пом'якшенні високочастотного резонансу TPSS. Цей результат підкреслює потенціал FLC як складного механізму управління підвищенням продуктивності систем в залізничних застосуваннях, демонструючи його перевагу над традиційними методами управління. Дослідження сприяє проливанню світла на інноваційні підходи до оптимізації управління та ефективності мережевих перетворювачів на основі LCL-фільтрів у системах високошвидкісних поїздів.* Бібл. 31, табл. 2, рис. 16.

Ключові слова: **мережевий перетворювач, LCL-фільтр, гармоніки, якість електроенергії, контролер нечіткої логіки, моделювання, високошвидкісна залізниця.**

1. **Introduction** High-speed rail frequently employs AC-DC-AC traction converters featuring Pulse Width Modulation (PWM) within electric units. This is done so as to enhance the energy quality and dynamic performance of railway electric systems [1], nevertheless, the presence of high-order harmonics is a common occurrence in railway electric networks, resulting in the challenge of high-frequency resonances [2, 3]. These harmonics give rise to a range of issues, including increased errors and disturbances, torque surges, thereby affecting the overall performance of the traction network [4]. Two primary strategies are commonly explored to tackle the issue of high-frequency harmonics in high-speed trains: one involves addressing the matter within the traction electrical system, meanwhile, the other aspect concentrates on the drive unit of high-speed trains.

The predominant research emphasis has been on mitigating harmonics within the traction system, with many scholars opting for the use of passive filters to alter the impedance of harmonics in this system [5]. In order to improve power quality, a grid-connected voltage source converter has incorporated an LCL-type filter, renowned for its superior high-frequency harmonic attenuation in comparison to conventional L-type filters. LCL filters find extensive use in grid-connected converters [6, 7] and front-active rectifiers [8, 9].

Comprehensive design procedures for a single-phase converter with an LCL filter were extensively discussed in [10, 11]. In addition, LCL filters often produce resonance peaks that endanger the stability of the grid-connected voltage link converter and impair the reliable operation of the traction power system.

Therefore, developing controllers suitable for LCL type single-phase converters faces huge challenges. Traditional PI linear controllers are usually used for grid-side converters of high-speed railways [12, 13]. However, the process of adjusting the PI parameters in the voltage or current control loop can be a problem, as incorrect settings

may result in undesired low-frequency oscillations in traction networks. In order to overcome this issue, various advanced nonlinear control techniques like model predictive control [14] and sliding mode control [15] were proposed in order to improve the dynamic behavior of systems. Nonetheless, implementing and adjusting parameters for these controllers in real-world scenarios can be difficult due to the presence of unknown parameters, complex structures and intricate mathematical models.

Fuzzy logic-based control has demonstrated effectiveness in various industrial applications [16, 17], owing to its heuristic nature, simplicity and efficiency for the utilization of fuzzy logic-based control has shown effectiveness in diverse industrial applications [16, 17], due to its simplicity, heuristic nature and efficiency for both linear and nonlinear systems. By utilizing linguistic variable knowledge, an intelligent fuzzy controller can be developed without the need for a complex mathematical model of the system. This not only reduces computation time but also improves the transient response characteristics of the system [18, 19]. However, designing an effective fuzzy controller in order to enhance the performance of a plant remains a challenging task, often requiring multiple trial-and-error procedures based on computer simulations.

As a solution, a proposed approach involves a simplified structure for the Fuzzy Logic Controller (FLC). Previous studies on line-side converters in high-speed railways have mainly focused on various aspects of controller design, including dynamic performance, stability analysis, and the mitigation of high-order harmonics [20-24].

Introducing a model predictive control for line-side traction rectifiers has demonstrated superior performance in suppressing high-order harmonics compared to traditional PI controllers. Another innovative method involves utilizing a nonlinear controller with active disturbance rejection control, aiming at optimizing the load characteristics of the train rectifier and reducing harmonics [25].

The application of the harmonic transfer function was employed to examine the stability of oscillating voltage fluctuation and controller performance [26]. Additionally, a combined predictive and extended state observer-based control system was proposed to mitigate voltage oscillations and reducing current distortions on both the train and network sides [27]. Some researchers have suggested a passivity-based control model for traction rectifiers so as to enhance both dynamic and static characteristics [28].

While these analytical methods have exhibited certain enhancements in controller performance, they heavily rely on precise mathematical models and a multitude of unknown parameters, often challenging to ascertain in practical applications. Despite the challenges associated with modern intelligent controller design, it is evident that existing control methods possess limitations. Specifically, they struggle to eradicate high-frequency harmonics, attain optimal system performance, and adjust control parameters. This limitation may impede the broader adoption of single-phase traction converters with LCL filters, consequently hindering advancements in railway electric systems. Notably, only a few endeavors have been made to explore the effectiveness of a fuzzy logic-based controller in electric drive applications [29, 30].

For high-speed railway line-side converters, the FLC emerges as a promising solution, eliminating the necessity for a detailed mathematical model of the system. Furthermore, it introduces a transparent physical approach to the control base in the closed loop, deviating from the use of cumbersome rings by others, implying an improvement in computational efficiency.

The goal of the paper is to devise a precise controller utilizing fuzzy logic control for a single-phase traction converter equipped with an LCL filter, with the aim of enhancing energy quality and mitigating undesired harmonic distortions within the railway traction power supply system.

2. System topology. A standard configuration for a high-speed railway traction power supply system is visually depicted in Fig. 1, offering a clear representation of the system. In this diagram the three-phase 220 kV utility undergoes a step-down transformation within an electrical substation to become two single-phase 27.5 kV feeders. This transformation is crucial for providing power to the all-parallel autotransformer-fed network through a V/x structure traction transformer.

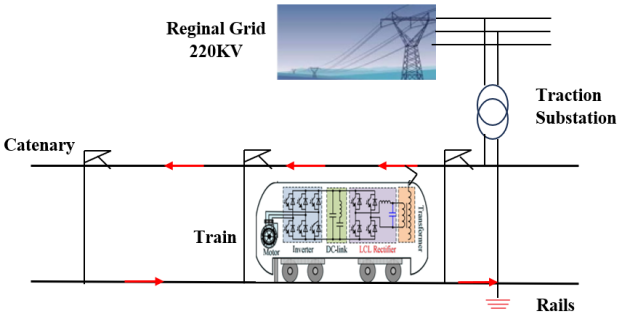

Fig. 1. Typical power-supply system for high-speed railway

Figure 2 illustrates a simplified diagram that showcases the positioning of the electrical train within the traction network system, in which: Z_{ss} is the feeder substation's equivalent impedance; i_T is the electric train's current; l_1 is the separation or gap between the electric train and the substation; l_2 is the distance between the electric train and endpoint of the feeder section.

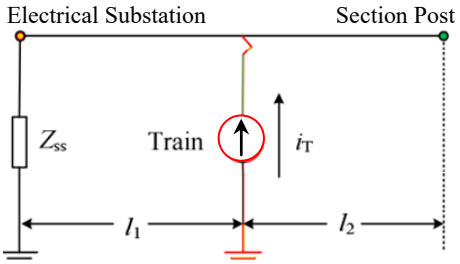

Fig. 2. The electrical train location diagram in the traction network system

This diagram incorporates various components such as communication wires, feeders, protection wires, rail and integrated grounding wires. The methodology used to create this diagram has been described in [31]. In this representation, the electrical train load is conceptually equated to a current source that contains harmonics.

Using the equivalent π-circuit model for multi-conductor transmission lines, Fig. 3 depicts the traction power network, in which: $Z_{T'1}$ and $Y_{T'1}$ are the impedance and admittance from the train to the substation; $Z_{T'2}$ and $Y_{T'2}$ are the impedance and admittance toward the supplying segment termination. The expressions for these values are:

$$\begin{cases} Z_{T'1} = \dfrac{Z_0(\cos\gamma l_1 - 1)}{\sin\gamma l_1}; \quad Y_{T'1} = \dfrac{\sin\gamma l_1}{Z_0}; \\ Z_{T'2} = \dfrac{Z_0(\cos\gamma l_2 - 1)}{\sin\gamma l_2}; \quad Y_{T'2} = \dfrac{\sin\gamma l_2}{Z_0}, \end{cases} \tag{1}$$

where γ, Z_0 are the unit-length propagation constant and characteristic impedance of the contact line, respectively. These parameters can be mathematically expressed as:

$$\begin{cases} Z_0 = \sqrt{Z'/Y'}; \\ \gamma = \sqrt{Z'Y'}, \end{cases} \tag{2}$$

where Z', Y' illustrate the impedance and admittance per unit length for the contact line, respectively.

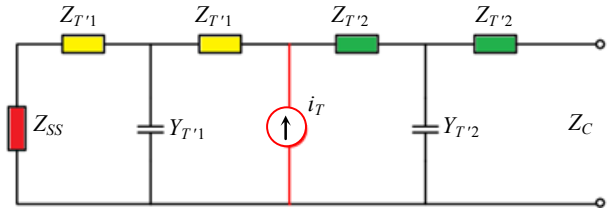

Fig. 3. Representation of equivalent traction network using topology of a π-circuit

When viewed from the train's electric system within the traction network, the parallel input impedance (Z_{pa}) formulation for the traction network can be expressed as:

$$Z_{Pa} = \frac{Z_0 \cos\gamma(l - l_1)(Z_{ss}\cos\gamma l_1 + Z_0 \sin\gamma l_1)}{Z_{ss}\sin\gamma l + Z_0 \cos\gamma l}. \tag{3}$$

The overall extent of the contact line, denoted as l (sum of l_1 and l_2), influences the parallel resonance in the traction network. The system exhibits parallel resonance when the denominator in (3) becomes 0, leading to the maximum impedance (Z_{pa}). The resonance condition is expressed as follows:

$$Z_{ss}\sin\gamma l + Z_0 \cos\gamma l = 0. \tag{4}$$

Given that γl is significantly less than 1, it is valid to approximate $\tanh(\gamma l)$ as ≈l, leading to the simplification as:

$$j\omega L_{ss} = \frac{-1}{j\omega C_c l} = \frac{-1}{j\omega C}, \tag{5}$$

where L_{ss} is the internal equivalent inductance of the electrical supply substation ($Z_{ss}=j\omega L_{ss}$); C_c is the distributed capacitance per unit extent of the contact line; C is the overall capacitance along the contact line.

The frequency of parallel resonance f_{pr} is:

$$f_{pr} = \frac{1}{2\pi\sqrt{L_{ss}C}}. \tag{6}$$

The resonance in the traction power network is a parallel resonance involving the equivalent inductor of the electric supply substation and the distributed capacitance across the multi-conductor transmission line. The resonance frequency is determined by the inherent properties of the traction network and remains unaffected by the electric train's location [32].

3. The LCL-type converter analysis. Figure 4 illustrates the unit equivalent to the traction drive for a high-speed locomotive, featuring a single-phase LCL-type converter topology on the grid side. In each power unit, line-side converters connect to the DC-link and incorporate an LCL-type passive filter. The traction transformer is idealized; L_g is the comparable leakage inductance on the secondary side; C_d is the DC-link capacitor; V_{dc} is the voltage on DC-link; R_L is the load equivalent for the traction inverter-motor drive system.

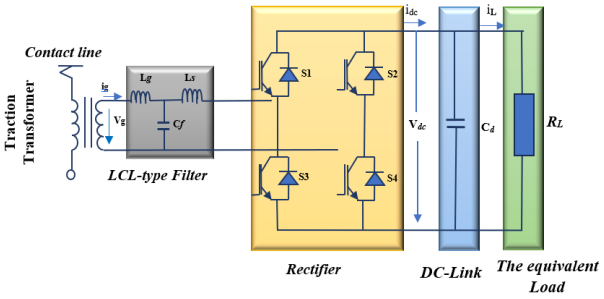

Fig. 4. Equivalent circuit of LCL-type rectifiers on the single-phase line side in every propulsion unit of a high-speed train

3.1. Designing and modeling LCL filters and their parameters. The inductance on the converter side L_s is usually determined based on the acceptable maximum converter current ripple ($\Delta i_{\max}$), typically ranging from 30-40 % of the rated current level. Therefore, the constraint condition for the inductance L_s can be expressed as:

$$L_s \geq \frac{u_{dc}}{8 f_s \Delta i_{\max}}, \tag{7}$$

where f_s is the switching frequency of the converter guides the selection of filter capacitance C_f.

Balancing high-frequency harmonics suppression and managing reactive power at the primary frequency is crucial [33]. To meet allowable reactive power, capacitance C_f can be calculated using (8), particularly at the primary frequency:

$$C_f \leq \beta \frac{P_n}{2\pi f_n U_s^2}, \tag{8}$$

where P_n is the specified power of the converter; β is the coefficient constrained to be under 5 %; f_n is the primary frequency of the grid voltage.

The design of the grid-side inductor L_g involves leveraging the proportion of high-order current on the converter side to that on the grid side. Due to unipolar PWM in a single-phase converter, emphasis is on high-order harmonics around double the switching frequency. Assuming no high-frequency components in the grid voltage, the LCL filter at double the switching frequency is addressed, as illustrated in Fig. 5.

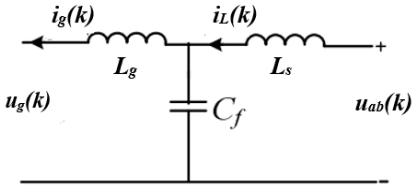

Fig. 5. Model of LCL filter

In Fig. 5 the transfer functions describing the relationship between u_{ab} and i_L, as well as i_g, can be articulated as:

$$\begin{cases} \dfrac{u_{ab}(k)}{i_L(k)} = \dfrac{j\omega_k L_s + j\omega_k L_g C_f - j\omega_k^3 L_f L_g C_f}{1 - j\omega_k^2 L_g C_f}; \\ \dfrac{u_{ab}(k)}{i_g(k)} = j\omega_k L_s - j\omega_k L_g - j\omega_k^3 L_s L_g C_f, \end{cases} \tag{9}$$

where ω_k is the twice angular frequency of switching.

Consequently, the calculation of the ratio between harmonic components on the grid-side current and high-order harmonic current on the inverter side can be determined as:

$$\sigma = \frac{i_g(k)}{i_L(k)} = \frac{1}{\left|1-\omega_k^2 L_g - C_f\right|}, \quad (10)$$

where the permissible ripple amplitude in the converter current set between 30 % to 40 % of the rated current, choosing σ at 15 % magnitude ensures a maximum fluctuation in grid-side current of around 5 %.

Consequently, the potential range for L_g can be inferred as:

$$L_g > \frac{23}{12\omega_k^2 C_f}. \quad (11)$$

In conclusion, the values of the inductor and capacitor need recalibration so as to align with the permissible design parameter range for the resonant frequency f_r. This study ensures that the resonant frequency f_r of the LCL filter is confined within the specified range:

$$5f_n < f_r < f_s. \quad (12)$$

The filter parameters specified in Table 1.

4. Control block diagram. Figures 6, 7 depict the control diagrams using a PI controller and a FLC, respectively. Table 1 presents the values for the single-phase traction converter with LCL filter parameters.

Table 1

System parameters

Parameters	Value
Contact-line voltage V_g, V	1550
Voltage across the DC-link $V_{dc\text{-}link}$, V	3000
Capacitor of the DC-link C_d, μF	3000
Frequency of switching f_s, Hz	550
Primary frequency f, Hz	50
LCL-type filter L_g, mH	1.3
Inductance on the converter side L_s, mH	1.6
Filter capacitance C_f, μF	125
Load resistor R_L, Ω	20

4.1. Control diagram with PI controller. Figure 6 shows the control scheme of the LCL rectifier based on PI controller, in which V_{dc} is the output voltage across the DC-link, where the initial block denotes V_{ref}. The regulator calculates the discrepancy between the reference and actual voltages, forming the input for the PI control unit. The output current from the PI regulator, combined with $\cos\omega t$ from the phase-locked loops (PLL) block, serves as the input for the 2nd block. The 3rd block represents the error from comparing the previous two values.

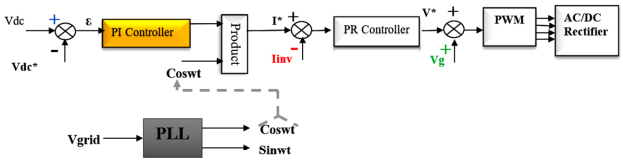

Fig. 6. Control scheme of the LCL rectifier based on PI controller

The output value (PR) from the proportional resonant controller (PR) unit becomes the voltage reference V_{ref}, added to V_{grid}. This resultant value is used in PWM generation for driver signals in the power electronic IGBT rectifier with a LCL filter, as shown in Fig. 6. The summarized mathematical equation for the system is:

$$I_{ref} = K_p(V_{dcref} - V_{dc}) + K_I \int (V_{dcref} - V_{dc})\mathrm{d}t. \quad (13)$$

4.2. Control diagram with FLC. Figure 7 shows the control scheme of the LCL rectifier based on FLC.

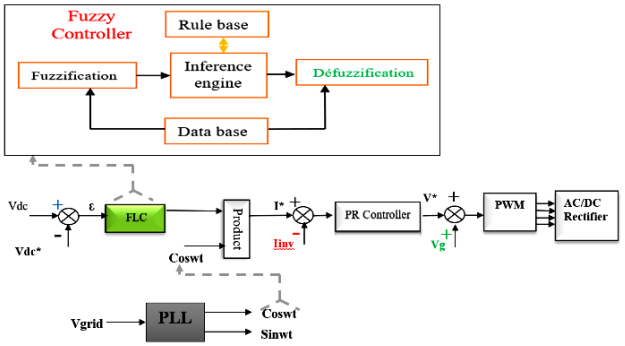

Fig. 7. Control scheme of the LCL rectifier based on FLC

A fuzzy control system leveraging fuzzy logic, evaluates input values in analog form using Boolean variables with continuous values ranging from 0 to 1. This contrasts with classical or digital logic, which operates on discrete values of either 1 or 0. The fuzzy controller consists of 3 stages: fuzzification, where inputs are converted into fuzzy representations using predefined membership functions; the rule-based inference system, which generates a fuzzy response based on linguistically defined rules; and defuzzification, converting the fuzzy response back into a crisp output. The design employs the Fuzzy Logic Toolbox in MATLAB/Simulink.

The inference engine in fuzzy logic, using Mamdani's method, connects membership functions to rules, generating fuzzy output. Defuzzification is the reverse process, transforming a fuzzy quantity into a precise value. In this application, the centroid method computed the result of the FLC, particularly the reference current in Table 2.

Table 2

Rule base of FLC

↓de/e→	NB	NS	Z	PS	PB
NB	NB	NB	NB	NS	Z
NS	NB	NB	NS	Z	PS
Z	NB	NS	Z	PS	PB
PS	NS	Z	PS	PB	PB
PB	Z	PS	PB	PB	PB

The inference engine is crucial in fuzzy logic, linking membership functions and fuzzy rules to generate the fuzzy output using Mamdani method. Defuzzification is the reverse process, transforming a fuzzy quantity into a precise value. In this application, the center of gravity method determined the output of the FLC, particularly the reference V, as shown in Fig. 8, illustrating the surface of fuzzy rules.

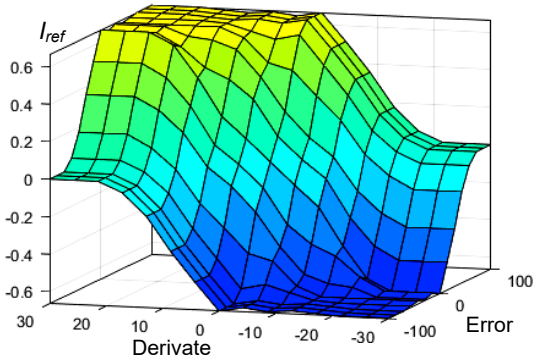

Fig. 8. Fuzzy rules surface

5. Results and comparison. Figures 9, 10 depict simulated waveforms of the DC-link voltages (V_{dc}), utilizing both the PI controller and the FLC, respectively. The observation highlights that the FLC reduces ripples and distortions in the capacitor voltage to a certain extent, while reducing the stabilization time to a value of $t = 0.1$ s compared to the PI controller, where the stabilization time is higher ($t = 0.6$ s), hindering the system's performance.

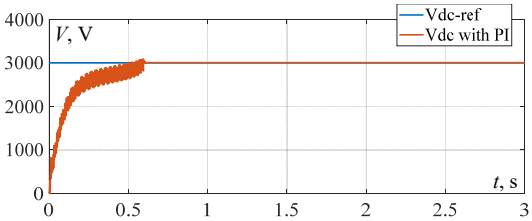

Fig. 9. The simulated waveforms of DC-link voltages based on PI controller

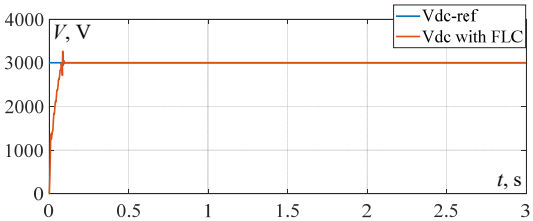

Fig. 10. The simulated waveforms of DC-link voltages based on FLC

This result indicates that the FLC brings a significant improvement in reducing fluctuations and distortions in the capacitor voltage, contributing to a faster and more stable system response. In comparison, the PI controller exhibits inferior performance with a longer stabilization time, which may compromise the overall system performance. These findings underscore the effectiveness of the FLC in enhancing dynamic response and the quality of the voltage across the DC-link in the considered converter.

Figures 11, 12 unveil the simulated voltage waveforms V_g of grid-side voltage during the functioning of a single-phase LCL rectifier using PI and FLCs, respectively. Examination of these figures reveals a significant disparity in the high-order harmonic components in the LCL rectifier with both controllers.

It is clearly evident that under the regulation by the PI controller, the voltage V_g exhibits more pronounced high-order harmonic components compared to those observed in the LCL rectifier operating with the FLC. This observation highlights the remarkable ability of the LCL converter topology with the FLC to significantly attenuate high-order harmonic resonance.

It is crucial to note that this enhanced harmonic attenuation capability offers substantial advantages in the context of power quality, thereby contributing to the stability of the traction power system. These results underscore the notable effectiveness of the FLC in reducing harmonics in comparison to the PI controller, suggesting that the adoption of the FLC could constitute a significant improvement in LCL rectifier applications, especially when it is crucial to effectively suppress high-order harmonic resonance.

Figures 13, 14 depict simulated waveforms of the grid-side current I_g of the LCL-type converter with PI and FLCs, respectively. The ability to eliminate high-frequency harmonics proves to be a crucial factor in the evaluation of filters and control systems. Following the comparison between Fig. 13, 14 it is noticed that the grid-side current is distorted, especially during the period 0–0.2 s, with higher harmonics from the PI controller compared to the FLC.

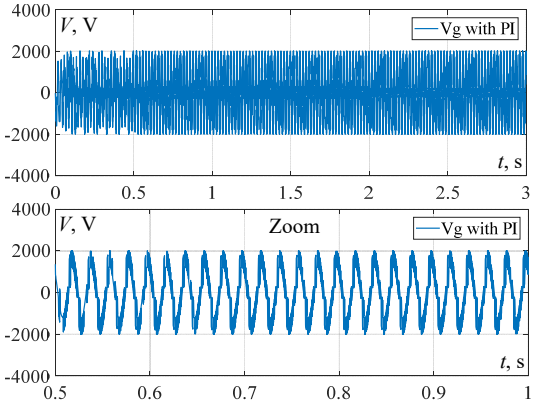

Fig. 11. The simulated waveforms of the grid-side voltage V_g using the PI controller

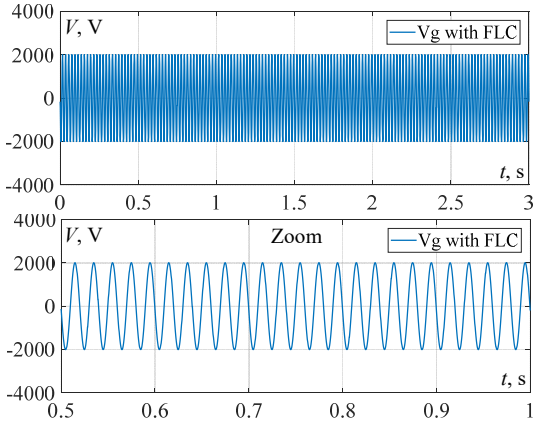

Fig. 12. The simulated waveforms of the grid-side voltage V_g using the FLC

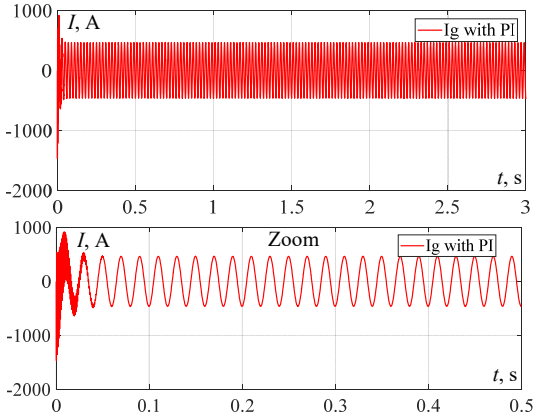

Fig. 13. The simulated waveforms of the grid-side current (I_g) using the PI controller

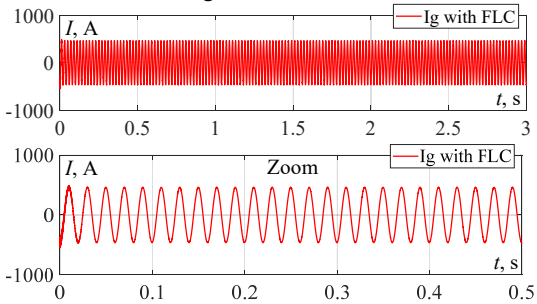

Fig. 14. The simulated waveforms of the grid-side current (I_g) using the FLC

This observation suggests that the attenuation of low-order harmonics operates effectively for the FLC, and low-order harmonics exhibit no significant impact influencing the grid-side current. This conclusion is corroborated by the results obtained from Fast Fourier Transform (FFT) analysis.

An examination of the results highlights the superior performance of the FLC in terms of harmonic reduction and waveform maintenance of the grid-side current, particularly during the critical period 0–0.2 s. These observations indicate that the choice of the FLC could represent a significant improvement in LCL-type converter applications, demonstrating increased effectiveness in suppressing harmonic distortions.

FFT algorithm is employed to assess the harmonic order within the grid-side current and THD of said current in a single-phase LCL converter utilizing PI and FLCs. THD measurements are contrasted for the PI and FLCs, as illustrated in Fig. 15, 16.

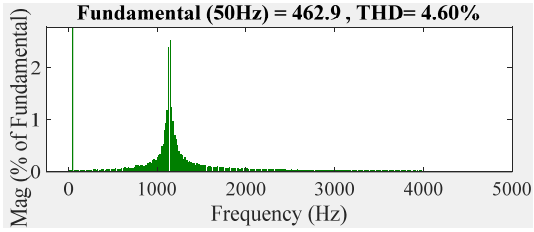

Fig. 15. The harmonic spectrum of the simulated grid-side current utilizing the PI controller

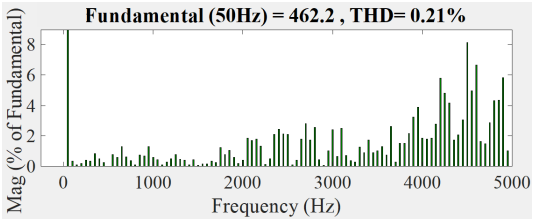

Fig. 16. The harmonic spectrum of the simulated grid-side current utilizing the FLC

Figure 15 displays the THD measurement results for the PI controller, yielding a value of 4.6 %. Conversely, Fig. 16 illustrates the corresponding results for the FLC, showing a notably reduced value of 0.21 %. These values fall well below the critical threshold of 5 %, aligning with harmonic standards.

This analysis demonstrates that the LCL filter ensures satisfactory compliance with harmonic standards, guaranteeing that the THD is below 5 %. Specifically, the results highlight the enhanced effectiveness of the FLC in harmonic suppression, particularly for high-frequency switching sub-harmonics. These findings underscore the notion that the implementation of the FLC represents a significant improvement for the LCL converter, notably ensuring a substantial reduction in THD.

Conclusions. A topological investigation and a mathematical model have been undertaken for the traction power supply system and the circuitry of single-phase line-side LCL-type rectifiers in each power unit of a high-speed train.

The control system aims at addressing high-order harmonic resonance in traction converter systems, particularly focusing on attenuating high-order harmonics in single-phase LCL PWM rectifiers. When guided by a Fuzzy Logic Controller (FLC), these rectifiers efficiently eliminate high-order harmonics in train traction drive systems. This approach, unlike conventional control units with a PI controller, effectively avoids stimulating high-frequency resonance.

The proposed method exhibits notable characteristics such as heightened robustness and autonomy from intricate system parameters. The simplicity and efficiency of the FLC distinguish it, suitable for both linear and nonlinear systems. Its intelligent control implementation does not require an intricate system model, reducing computation time and enhancing response dynamics.

The study conducts a comprehensive comparative analysis of harmonic suppression performance in the LCL converter, comparing its performance with a traditional PI controller to the proposed FLC. Analytical scrutiny and a THD study emphasize the efficacy of the FLC-controlled transformer, affirming its role in ensuring high-quality dynamic performance in traction systems.

Conflict of interest. The authors of the article declare that there is no conflict of interest.

REFERENCES

1. Liu Y., Xu J., Shuai Z., Li Y., Cui G., Hu S., Xie B. Passivity-based decoupling control strategy of single-phase LCL-type VSRs for harmonics suppression in railway power systems. *International Journal of Electrical Power & Energy Systems*, 2020, vol. 117, art. no. 105698. doi: https://doi.org/10.1016/j.ijepes.2019.105698.

2. Djazia K., Sarra M. Improving the quality of energy using an active power filter with zero direct power command control related to a photovoltaic system connected to a network. *Electrical Engineering & Electromechanics*, 2023, no. 5, pp. 20-25. doi: https://doi.org/10.20998/2074-272X.2023.5.03.

3. Aissaoui M., Benidir M., Bouzeria H., Berroum F., Ras A.C., Mammeri I. Analysis of harmonic resonance in traction power supply system. *2022 2nd International Conference on Advanced Electrical Engineering (ICAEE)*, 2022, pp. 1-5. doi: https://doi.org/10.1109/ICAEE53772.2022.9962039.

4. Lv X., Wang X., Che Y., Fu R. Eigenvalue-Based Harmonic Instability Analysis of Electrical Railway Vehicle-Network System. *IEEE Transactions on Transportation Electrification*, 2019, vol. 5, no. 3, pp. 727-744. doi: https://doi.org/10.1109/TTE.2019.2929406.

5. Balakishan P., Chidambaram I.A., Manikandan M. Improvement of power quality in grid-connected hybrid system with power monitoring and control based on internet of things approach. *Electrical Engineering & Electromechanics*, 2022, no. 4, pp. 44-50. doi: https://doi.org/10.20998/2074-272X.2022.4.06.

6. Han Y., Yang M., Li H., Yang P., Xu L., Coelho E.A.A., Guerrero J.M. Modeling and Stability Analysis of LCL-Type Grid-Connected Inverters: A Comprehensive Overview. *IEEE Access*, 2019, vol. 7, pp. 114975-115001. doi: https://doi.org/10.1109/ACCESS.2019.2935806.

7. Gurrola-Corral C., Segundo J., Esparza M., Cruz R. Optimal LCL-filter design method for grid-connected renewable energy sources. *International Journal of Electrical Power & Energy Systems*, 2020, vol. 120, art. no. 105998. doi: https://doi.org/10.1016/j.ijepes.2020.105998.

8. Jiang S., Liu Y., Liang W., Peng J., Jiang H. Active EMI Filter Design With a Modified LCL-LC Filter for Single-Phase Grid-Connected Inverter in Vehicle-to-Grid Application. *IEEE Transactions on Vehicular Technology*, 2019, vol. 68, no. 11, pp. 10639-10650. doi: https://doi.org/10.1109/TVT.2019.2944220.

9. Tang W., Ma K., Song Y. Critical Damping Ratio to Ensure Design Efficiency and Stability of LCL Filters. *IEEE Transactions on Power Electronics*, 2021, vol. 36, no. 1, pp. 315-325. doi: https://doi.org/10.1109/TPEL.2020.3000897.

10. Rasekh N., Hosseinpour M. LCL filter design and robust converter side current feedback control for grid-connected Proton Exchange Membrane Fuel Cell system. *International Journal of Hydrogen Energy*, 2020, vol. 45, no. 23, pp. 13055-13067. doi: https://doi.org/10.1016/j.ijhydene.2020.02.227.
11. Milbradt D.M.C., Hollweg G.V., de Oliveira Evald P.J.D., da Silveira W.B., Gründling H.A. A robust adaptive One Sample Ahead Preview controller for grid-injected currents of a grid-tied power converter with an LCL filter. *International Journal of Electrical Power & Energy Systems*, 2022, vol. 142, art. no. 108286. doi: https://doi.org/10.1016/j.ijepes.2022.108286.
12. Al-Barashi M., Meng X., Liu Z., Saeed M.S.R., Tasiu I.A., Wu S. Enhancing power quality of high-speed railway traction converters by fully integrated T-LCL filter. *IET Power Electronics*, 2023, vol. 16, no. 5, pp. 699-714. doi: https://doi.org/10.1049/pel2.12415.
13. Dey P., Sumpavakup C., Kirawanich P. Optimal Control of Grid Connected Electric Railways to Mitigate Low Frequency Oscillations. *2022 Research, Invention, and Innovation Congress: Innovative Electricals and Electronics (RI2C)*, 2022, pp. 70-75. doi: https://doi.org/10.1109/RI2C56397.2022.9910283.
14. Xue J.-Z., Zhao T., Bu N., Chen X.-L., Zhang B. Speed tracking control of high-speed train based on adaptive control and linear active disturbance rejection control. *Transactions of the Institute of Measurement and Control*, 2023, vol. 45, no. 10, pp. 1896-1909. doi: https://doi.org/10.1177/01423312221146600.
15. Tasiu I.A., Liu Z., Wu S., Yu W., Al-Barashi M., Ojo J.O. Review of Recent Control Strategies for the Traction Converters in High-Speed Train. *IEEE Transactions on Transportation Electrification*, 2022, vol. 8, no. 2, pp. 2311-2333. doi: https://doi.org/10.1109/TTE.2022.3140470.
16. Zhao L., Yin Z., Yu K., Tang X., Xu L., Guo Z., Nehra P. A Fuzzy Logic-Based Intelligent Multiattribute Routing Scheme for Two-Layered SDVNs. *IEEE Transactions on Network and Service Management*, 2022, vol. 19, no. 4, pp. 4189-4200. doi: https://doi.org/10.1109/TNSM.2022.3202741.
17. Woźniak M., Zielonka A., Sikora A. Driving support by type-2 fuzzy logic control model. *Expert Systems with Applications*, 2022, vol. 207, art. no. 117798. doi: https://doi.org/10.1016/j.eswa.2022.117798.
18. Kambalimath S., Deka P.C. A basic review of fuzzy logic applications in hydrology and water resources. *Applied Water Science*, 2020, vol. 10, no. 8, art. no. 191. doi: https://doi.org/10.1007/s13201-020-01276-2.
19. Paranchuk Y.S., Shabatura Y.V., Kuznyetsov O.O. Electromechanical guidance system based on a fuzzy proportional-plus-differential position controller. *Electrical Engineering & Electromechanics*, 2021, no. 3, pp. 25-31. doi: https://doi.org/10.20998/2074-272X.2021.3.04.
20. Ali Moussa M., Derrouazin A., Latroch M., Aillerie M. A hybrid renewable energy production system using a smart controller based on fuzzy logic. *Electrical Engineering & Electromechanics*, 2022, no. 3, pp. 46-50. doi: https://doi.org/10.20998/2074-272X.2022.3.07.
21. Muthubalaji S., Devadasu G., Srinivasan S., Soundiraraj N. Development and validation of enhanced fuzzy logic controller and boost converter topologies for a single phase grid system. *Electrical Engineering & Electromechanics*, 2022, no. 5, pp. 60-66. doi: https://doi.org/10.20998/2074-272X.2022.5.10.
22. Khatir A., Bouchama Z., Benaggoune S., Zerroug N. Indirect adaptive fuzzy finite time synergetic control for power systems. *Electrical Engineering & Electromechanics*, 2023, no. 1, pp. 57-62. doi: https://doi.org/10.20998/2074-272X.2023.1.08.
23. Gopal Reddy S., Ganapathy S., Manikandan M. Power quality improvement in distribution system based on dynamic voltage restorer using PI tuned fuzzy logic controller. *Electrical Engineering & Electromechanics*, 2022, no. 1, pp. 44-50. doi: https://doi.org/10.20998/2074-272X.2022.1.06.
24. Ikhe A., Pahariya Y. Voltage regulation using three phase electric spring by fuzzy logic controller. *Electrical Engineering & Electromechanics*, 2023, no. 4, pp. 14-18. doi: https://doi.org/10.20998/2074-272X.2023.4.02.
25. Goyal D.K., Birla D. A comprehensive control strategy for power quality enhancement in railway power system. *International Journal of Advanced Technology and Engineering Exploration*, 2023, vol. 10, no. 106, pp. 1123-1137. doi: https://doi.org/10.19101/IJATEE.2023.10101018.
26. Liu Y., Yang Z., Wu X., Lan L., Lin F., Su H., Huang J. Adaptive Threshold Adjustment Strategy Based on Fuzzy Logic Control for Ground Energy Storage System in Urban Rail Transit. *IEEE Transactions on Vehicular Technology*, 2021, vol. 70, no. 10, pp. 9945-9956. doi: https://doi.org/10.1109/TVT.2021.3109747.
27. Alekhya G.B.S., Shashikanth K., Prasad M.A. Risk assessment of cost overrun using fuzzy logic model. *Materials Today: Proceedings*, 2022, vol. 62, pp. 1803-1810. doi: https://doi.org/10.1016/j.matpr.2021.12.415.
28. Moaveni B., Rashidi Fathabadi F., Molavi A. Fuzzy control system design for wheel slip prevention and tracking of desired speed profile in electric trains. *Asian Journal of Control*, 2022, vol. 24, no. 1, pp. 388-400. doi: https://doi.org/10.1002/asjc.2472.
29. Pradhan R.K., Sahu C.K. Single-input Fuzzy PI Controller for Traction Line-Side Converter of High Speed Railway. *2021 12th International Conference on Computing Communication and Networking Technologies (ICCCNT)*, 2021, pp. 1-6. doi: https://doi.org/10.1109/ICCCNT51525.2021.9579548.
30. Al-Faris M., Chiverton J., Ndzi D., Ahmed A.I. Vision Based Dynamic Thermal Comfort Control Using Fuzzy Logic and Deep Learning. *Applied Sciences*, 2021, vol. 11, no. 10, art. no. 4626. doi: https://doi.org/10.3390/app11104626.
31. Liu Y., Xu J., Shuai Z., Li Y., Peng Y., Liang C., Cui G., Hu S., Zhang M., Xie B. A Novel Harmonic Suppression Traction Transformer with Integrated Filtering Inductors for Railway Systems. *Energies*, 2020, vol. 13, no. 2, art. no. 473. doi: https://doi.org/10.3390/en13020473.
32. Song W., Jiao S., Li Y.W., Wang J., Huang J. High-Frequency Harmonic Resonance Suppression in High-Speed Railway Through Single-Phase Traction Converter With LCL Filter. *IEEE Transactions on Transportation Electrification*, 2016, vol. 2, no. 3, pp. 347-356. doi: https://doi.org/10.1109/TTE.2016.2584921.
33. Gervasio F.A., Bueno E., Mastromauro R.A., Liserre M., Stasi S. Voltage control of microgrid systems based on 3lnpc inverters with LCL-filter in islanding operation. *2015 International Conference on Renewable Energy Research and Applications (ICRERA)*, 2015, pp. 827-832. doi: https://doi.org/10.1109/ICRERA.2015.7418527.

Received 22.09.2023
Accepted 03.11.2023
Published 02.03.2024

M. Aissaoui[1], *PhD Student,*
H. Bouzeria[1], *Doctor, Associate Professor,*
M. Benidir[1], *Professor,*
M.A. Labed[2], *PhD Student,*
[1] LITE Laboratory, Transportation Engineering Department, University of Constantine 1, Algeria,
e-mail: meryem.aissaoui@umc.edu.dz (Corresponding Author); bouzeria.hamza@umc.edu.dz; mohamed.benidir@umc.edu.dz
[2] LGEC Research Laboratory, Department of Electrical Engineering,
University of Constantine 1, Algeria,
e-mail: mohamedamir.labed@student.umc.edu.dz

How to cite this article:
Aissaoui M., Bouzeria H., Benidir M., Labed M.A. Harmonics suppression in high-speed railway via single-phase traction converter with an LCL filter using fuzzy logic control strategy. *Electrical Engineering & Electromechanics*, 2024, no. 2, pp. 16-22. doi: https://doi.org/10.20998/2074-272X.2024.2.03